

See discussions, stats, and author profiles for this publication at: <https://www.researchgate.net/publication/38052585>

# Rapid Determination of RNA Accessible Sites by Surface Plasmon Resonance Detection of Hybridization to DNA Arrays

ARTICLE *in* ANALYTICAL CHEMISTRY · NOVEMBER 2009

Impact Factor: 5.64 · DOI: 10.1021/ac9015962 · Source: PubMed

---

CITATIONS

16

---

READS

19

6 AUTHORS, INCLUDING:



**Matthew Lockett**

University of North Carolina at Chapel Hill

35 PUBLICATIONS 605 CITATIONS

SEE PROFILE



**Margaret F Phillips**

University of Wisconsin–Madison

6 PUBLICATIONS 177 CITATIONS

SEE PROFILE

Published in final edited form as:

*Anal Chem.* 2009 November 1; 81(21): 8949–8956. doi:10.1021/ac9015962.

## Rapid Determination of RNA Accessible Sites by Surface Plasmon Resonance Detection of Hybridization to DNA arrays

Joshua B. Mandir<sup>1,4</sup>, Matthew R. Lockett<sup>1,4</sup>, Margaret F. Phillips<sup>1</sup>, Hatim T. Allawi<sup>2</sup>, Victor I. Lyamichev<sup>2</sup>, and Lloyd M. Smith<sup>1,3,\*</sup>

<sup>1</sup>Department of Chemistry, University of Wisconsin-Madison

<sup>2</sup>Hologic, Inc. Madison, WI

<sup>3</sup>Genome Center of Wisconsin, University of Wisconsin-Madison

### Abstract

RNA accessible sites are the regions in an RNA molecule, which are available for hybridization with complementary DNA or RNA molecules. The identification of these accessible sites is a critical first step in identifying antisense-mediated gene suppression sites, as well as in a variety of other RNA-based analysis methods. Here, we present a rapid, hybridization-based, label-free method of identifying RNA accessible sites with surface plasmon resonance imaging (SPRi) on *in situ* synthesized oligonucleotide arrays prepared on carbon-on-metal substrates. The accessible sites of three pre-miRNAs, miRNA precursors of ~75 nt in length, were determined by hybridizing the RNA molecules to RNA-specific tiling arrays. An array comprised of all possible 6mer oligonucleotide sequences was also utilized in this work, offering a universal platform capable of studying RNA molecules in a high throughput manner.

### Introduction

The rich secondary and tertiary structure adopted by an RNA molecule leaves only a small portion of its sequence available for hybridization.<sup>1-4</sup> These hybridizable regions are termed RNA “accessible sites,”<sup>5</sup> and are thought to play an important role in RNA interference (RNAi). RNAi is a type of gene regulation occurring after transcription but prior to translation, and is responsible for modulating protein expression in cells.<sup>6,7</sup> Determining and targeting an RNA molecule's accessible sites, therefore, is an important first step in anti-sense gene suppression as well as in other RNA analysis methods such as primer extension and RT-PCR.

A variety of theoretical and experimental methods have been developed to probe RNA accessible sites. The experimental methods<sup>8,9</sup> tend to be time-consuming, labor-intensive, and due to their low-throughput nature are cost-prohibitive for screening a large number of RNA molecules. Computational methods have been developed to predict RNA folding patterns, providing a starting point to predict the accessible sites.<sup>10-16</sup> The folding programs commonly used rely on nearest-neighbor free energy approximations to determine the overall lowest energy conformation of the RNA molecule. Inaccuracies in the parameters employed as well as an exponential increase in the computational difficulty of the modeling process with

\*smith@chem.wisc.edu.

<sup>4</sup>These two authors contributed equally to this work

Supplementary Information Available:

Supplementary images (S1 – S4) as well as a detailed description of the oligonucleotide sequences contained in each of the arrays utilized in this work are presented (PDF). This material is available free of charge via the Internet at <http://pubs.acs.org>.

increasing RNA length often results in inadequate structure predictions to guide the experimental process.

Several groups have studied RNA structure utilizing oligonucleotide arrays. Oligonucleotide arrays provide a convenient means of monitoring many hybridization events in a parallel manner, providing a high throughput means of analyzing RNA accessible sites. One of the earliest such methods probed the RNA accessible sites of the tRNA<sup>phe</sup> molecule by synthesizing a DNA tiling array containing all possible 15mer perfect complements.<sup>17</sup> Recently, there has been a substantial effort to improve theoretical folding models with the information gained from such array-based hybridization experiments. Oligonucleotide arrays composed of combinations of 9mer<sup>18</sup> and 6mer<sup>19</sup> complements were fabricated and used to determine the accessible sites of a 249 nucleotide RNA molecule from the 3' end of the R2 retrotransposon from *Bombyx mori* and the S5 rRNA molecule from *E. coli*, respectively. The array-based hybridization data along with the results from melting curve experiments and enzymatic and chemical maps of the RNA molecules were used to design a complementary computer-based approach to evaluate the folding patterns predicted with nearest-neighbor free energy approximations. Additionally, high-density DNA arrays have been used to develop algorithms for predicting which structural effects in a folded RNA molecule promote and/or prohibit hybridization.<sup>20</sup>

The method described here focuses on the experimental determination of RNA accessible sites utilizing oligonucleotide arrays and differs from the above-mentioned work in three respects: the method of array fabrication utilized, the detection method utilized, and the universality of this platform to potentially probe many different RNA molecules on the same array.

The oligonucleotide arrays used in this work were fabricated using *in-situ*, light-directed synthetic methods to synthesize individual oligonucleotide features in a base-by-base manner.<sup>21,22</sup> Oligonucleotide arrays comprising up to 4122 features were synthesized using maskless array synthesis (MAS) technology, in which arrays are designed and synthesized through a series of computer-software controlled “virtual masks.” Here the term “feature” refers to a geographically distinct region on the array containing many copies of a single oligonucleotide sequence. MAS is an attractive alternative to arraying pre-synthesized oligonucleotides via spotting methods as it permits the end user to prepare a higher-density array with a greater diversity of sequences in less time and at a lower cost. Each oligonucleotide array was fabricated on recently developed carbon-on-metal substrates in which a thin layer of amorphous carbon is deposited onto a surface plasmon resonance (SPR)-active gold substrate.<sup>23</sup> The substrate has the chemical stability of carbon-based materials while preserving the optical properties of the gold thin film and its ability to support surface plasmons. The high stability of oligonucleotide arrays fabricated on this substrate permits multiple hybridization reactions to be performed on a single array.<sup>24</sup> This reduces artifacts arising from array-to-array variations as well as the costs incurred by the end-user.

A second feature of this method is that hybridization events can be monitored with SPR imaging (SPRi) techniques. SPR is a surface-sensitive method that allows interactions between molecules immobilized on a surface and analyte molecules in solution to be monitored in a real-time and label-free manner.<sup>25-27</sup> Numerous studies of biomolecular interactions have been performed with fixed-angle SPR imaging techniques on surfaces patterned with a variety of biomolecules such as DNA, RNA, proteins, and peptides.<sup>28</sup> The ability to detect biomolecule binding events without the use of labels provides two important advantages in developing a generalized method for monitoring RNA accessible sites: (1) the process of labeling and/or incorporating radioactive tags into RNA molecules and subsequent purification methods are eliminated and (2) studying native RNA molecules eliminates the concern that incorporation of reporter molecules may alter the overall structure.

Lastly, the combination of the MAS oligonucleotide array fabrication with the label-free detection capabilities of SPR compatible carbon substrates allows the fabrication of a single “universal array” that contains all possible 6mers. In principle, a single, universal array provides generalized accessible site information for RNA molecules of any sequence. This is in contrast to RNA-specific tiling arrays, which are comprised of oligonucleotide features that cover a single RNA molecule's sequence.<sup>29</sup>

Here, the accessible sites for three pre-micro RNA precursor molecules (pre-miR-155, pre-let-7a3, pre-let-7c, Table 1) ranging in length from 65 to 84 nucleotides (nt) were determined by hybridizing the RNA molecules to the oligonucleotide arrays described above. The method presented here allows RNA accessible sites to be determined within a few minutes, by simply incubating the oligonucleotide array with a solution of the unlabeled RNA molecule and monitoring hybridization with SPR imaging. Two types of arrays were designed and synthesized: three RNA-specific tiling arrays, in which the individual DNA elements of the array are the complements that correspond to those DNA sequences present in the RNA target, and a single universal array containing all possible 6mer oligonucleotides. RNA-specific tiling arrays were used to determine the accessible sites of each of the pre-micro RNA molecules and the universal array was used to determine the accessible sites of the pre-let-7a3 molecule. The pre-let-7a3 accessible sites obtained from the RNA-specific and the universal arrays were similar, demonstrating that the universal arrays provide results that are comparable in quality to those generated using the RNA-specific arrays.

## Materials and Methods

### Nucleic acids

Oligonucleotides used in this work are listed in Table 1 and were prepared using standard phosphoramidite chemistries by the UW-Madison Biotechnology Center (Madison, WI), Integrated DNA Technologies (Coralville, IA) and Dharmacon RNAi Technologies (Lafayette, CO).

### Surface Preparation

The fabrication of the carbon-on-metal substrates used in this work has been previously described in detail.<sup>23</sup> Briefly, 42.5nm gold films with a 2.0nm chromium underlayer were deposited onto high index glass (SF10, Schott Glass) substrates using an Angstrom Engineering Åmod metal evaporator. Next, 7.5nm of amorphous carbon was magnetron sputtered (Denton Vacuum) onto the substrates.

Prior to oligonucleotide array fabrication, each carbon-on-metal substrate was chemically functionalized using previously reported methods.<sup>23,30,31</sup> Each substrate was hydrogen-terminated, neat 9-decene-1-ol molecules were attached to the substrate via a UV photochemical reaction, and the substrates were thoroughly rinsed with ethanol and deionized (DI) water, dried under nitrogen and stored in a desiccator until needed.

### In situ oligonucleotide synthesis

Oligonucleotide arrays were fabricated using a previously described light-directed photographic synthesis method, which utilized maskless array synthesis (MAS) technology and allowed each oligonucleotide sequence to be synthesized in a base-by-base manner.<sup>22</sup> Syntheses were performed with oligonucleotide bases modified with a photolabile 3'-nitrophenylpropyloxycarbonyl (NPPOC)-protecting group (Sigma-Proligo) and a digital micromirror-based Biological Exposure and Synthesis System connected to a Perspective Biosystems Expedite Nucleic Acid Synthesis System. A detailed description of the synthesis conditions utilized in this work has been presented previously.<sup>23,31</sup>

Prior to array synthesis, a series of computer-generated “virtual masks” are designed on a LabView-based program; each mask corresponds to a step in the array synthesis. Virtual masks are projected onto the array via a digital micromirror device, commonly used in commercial LCD projectors. Before synthesis begins, an NPPOC-protected dT is coupled to the entire synthesis area. When the first virtual mask is displayed, ultraviolet light strikes the surface in the designated areas, removing the NPPOC protecting group. Next, the nucleotide of choice (NPPOC-protected dA, dC, dG, or dT) is introduced to the surface and coupled to the recently deprotected areas. This process repeats until all of the oligonucleotide features are synthesized.

### Array design

Three separate control oligonucleotide sequences were used throughout this work (Table 1) to determine the specificity and fidelity of each array. Specificity was determined by hybridizing fluorescently labeled, complementary DNA sequences to control sequences located on the array (Complement 1 to Control 1 and/or Complement 2 to Control 2). The fidelity was determined by a third control (Control 3), which was a Cy3-terminated dT feature. Controls 1-3 are commonly used in our laboratory to confirm the successful completion of array fabrication. A 10 dT spacer was used to separate every feature in each of the arrays from the surface, this has been shown to facilitate hybridization.<sup>32</sup>

Three RNA-specific tiling arrays were designed and fabricated (Figure 1), one for each of three the RNA sequences studied (pre-miR-155, pre-let-7a3, pre-let-7c in Table 1). Each tiling array steps through the complement of its respective RNA sequence one nucleotide at a time in the 5' → 3'-direction. Each of the tiling arrays were composed of 192  $\mu\text{m}$  × 192  $\mu\text{m}$  oligonucleotide features separated by 128  $\mu\text{m}$ .

The 534-feature pre-miR-155 array (pre-miR-155 RNA molecule, 65 nt, Table 1) contains three tiling subarrays with each 6mer, 8mer, and 12mer complementary sequence. Each subarray is in triplicate (516 features total) with 6 features for each of the three control sequences. The pre-let-7c and pre-let-7a3 arrays were designed in a similar fashion with the following differences.

In the pre-let-7c array the 6, 8, and 12mer subarrays are only in duplicate, Control 3 (5 features) and Control 1 (3 features) were used, and all lengths of perfect complement to the 3'- and 5'-termini were fabricated from monomers through 12mers. This design resulted in a 502-feature array. In the pre-let-7a3 array, 4, 5, 6, 8, and 12mer subarrays were fabricated in duplicate, Control 1 and 2 (3 features each) were used, and all lengths of perfect complements to the 3'- and 5'-termini were fabricated from monomers to 12mers. This design resulted in a 714-feature array. The pre-let-7a3 array employed a S18 Spacer group (Glen Research) between the 10 dT linker and the sequences of interest to investigate what impact, if any, the spacer region had on the binding seen in previous studies. No significant difference was observed when using the S18 Spacer.

A universal array (4122 total features) containing all possible 6mer combinations as well as Control 1 and 3 sequences (3 features of each) was fabricated. This array is termed universal as it can probe the hybridization of any RNA molecule. The universal array contained 96  $\mu\text{m}$  × 96  $\mu\text{m}$  oligonucleotide features with 48  $\mu\text{m}$  inter-feature spacing. Detailed information on the exact sequences synthesized for each array is provided in Supplementary Tables 1-4.

### SPR imaging experiments

An SPRImager II (GWC Technologies, Madison, WI) was used to monitor all the hybridization experiments. This instrument is described in detail elsewhere.<sup>33</sup> Briefly, a collimated white light source is polarized with a near-infrared polarizer and directed onto a prism/substrate

assembly at a fixed angle, which is set to be slightly smaller than the SPR angle. The light reflected off the prism/substrate assembly is collected with a CCD camera after passing through a narrow band-pass filter centered at 800 nm. SPRi data were collected using software written in V++ 4.0 (Digital Optics). In a typical SPRi experiment a reference image is collected and subsequent time-dependent difference images are acquired by subtracting the reference image. The intensity changes in these images are reported in units of  $\Delta\%R$ , which correspond to the percent reflectivity change.

## Hybridization Experiments

In each hybridization experiment ~200 $\mu$ L RNA solution was recirculated with a peristaltic pump over the oligonucleotide array contained within an enclosed, 100 $\mu$ L flow cell, and whose hybridization was monitored by SPR imaging. Prior to introducing the RNA molecule to the array, buffer (7.5mM MgCl<sub>2</sub>, 10mM MOPS, pH 7.4 unless otherwise noted) was introduced and an initial (reference) SPR image obtained. Next, a solution containing the RNA molecule of interest was introduced into the flow cell and hybridization was monitored as a function of time. Hybridization to the array was monitored in real time with the SPR image collection software (V++) and was observed in less than one minute, which is the time required to fill the flow cell with the solution containing the RNA. After hybridization, a second image was collected. This final image of the array was collected approximately five minutes after the intensities of the hybridized features reached their maximum value (i.e. equilibrium was established).

## Data Analysis

Each hybridization experiment was analyzed in the following manner. Difference images were obtained by subtracting the SPR image after hybridization from the initial reference image. Hybridization to the array results in an increase in feature intensity. Accessible sites are defined as regions of the RNA molecule that hybridize to the oligonucleotide array. Here, an accessible site is defined as a region that hybridizes to an individual feature of the array with a signal increase (increase in reflectivity,  $\Delta\%R$ ) that is three times greater than the standard deviation of the background signal ( $3\sigma$ ). The background signal is the average intensity of the control features. If hybridization to a feature on the array results in an intensity change of less than  $3\sigma$ , it was considered to correspond to an inaccessible area on the RNA molecule.

## RNA Secondary Structure Predictions

Theoretically derived folding patterns for each of the RNA molecules were obtained using the software program Mfold.<sup>10,34</sup> The default settings (25°C, 1000mM NaCl) of the Mfold program were used in all structure predictions.

## Results and Discussion

The accessible sites of three individual RNA molecules (pre-miR-155, pre-let-7a3, and pre-let-7c, Table 1) were determined by hybridizing these molecules to their RNA-specific tiling arrays, which were *in situ* synthesized on carbon-on-metal substrates and hybridization monitored with SPR imaging. The accessible sites for the pre-let-7a3 RNA molecule were also determined by hybridizing the molecule to a universal array that is composed of all possible 6mer oligonucleotide sequences. The accessible sites for the pre-let-7a3 molecule determined from the RNA-specific and universal array were compared. The RNA molecules used in this study are microRNA precursors and were chosen because of their known secondary structures, which generally contain a two-turn intramolecular stem (~20 base pairs) with various bulges, loops, mismatches, and non-Watson-Crick base-pairing sites.<sup>35-36</sup>



The RNA molecules were hybridized to DNA molecules covalently attached to the carbon-on-metal substrates and monitored with SPRi, a label-free means of detecting biomolecule interactions on surfaces. In each SPRi experiment, a reference image of the surface was obtained prior to introducing the RNA molecule of interest. Next, the RNA molecule was introduced to the array and hybridization was monitored via a series of collected images. Difference images (image at time  $x$  – reference image) indicate hybridization events to specific array oligonucleotide features via signal intensity changes: as RNA binds to the surface, the reflectivity of that area increases, giving an increased light signal at the detector. This signal change is linearly proportional to the amount of material that binds to the surface, thus providing quantitative results.<sup>33,37</sup> Accessible sites were determined by comparing the intensity changes of hybridized array features with the intensity changes of the background, the portion of the array not containing DNA molecules. Intensity increases that were at least 3 times the standard deviation of the background intensity ( $3\sigma$ ) were attributed to specific hybridization, and thus deemed an accessible site. Accessible site maps of the 3 RNA molecules were generated using this  $3\sigma$  hybridization criteria and are the average of three independent experiments.

### Pre-miR-155 RNA-specific array

The pre-miR-155 (Table 1) RNA-specific array is a 534-feature tiling array composed of 6mer, 8mer, and 12mer complementary sequences. Figure 1a contains a diagram and reference image of the pre-miR-155 RNA-specific array. Figure 2a contains a difference image obtained after the pre-miR-155 RNA molecule was hybridized to the array. The 6mer regions of the array show hybridization ranging from oligonucleotide start position U30 to A45, and correspond to an accessible region of U30 to A50 (Figure 2b). The 8mer and 12mer regions show similar regions of hybridization, but are expanded and have higher signal intensity. Supplementary Figures S1a and S1b contain the accessible site maps obtained for the 8mer and 12mer oligonucleotide features, respectively. The significant increase in intensity for the 8 and 12mer regions also indicate a larger number of RNA molecules hybridized to the array and is attributed to an increased stability of duplex formation. The accessible site map obtained from the hybridization data for the 6mer probes is shown in Figure 2c, which matches the lowest-energy structure predicted by the Mfold software program.<sup>10</sup> The accessible site map shows binding from the 5'-side of the loop to the 3'-side of the stem.

A control experiment was performed to confirm that in the absence of secondary structure, uniform and equal hybridization would be obtained for all surface-bound complements present in the molecule. The mature miR-155 RNA is a 21mer, corresponding to bases U4-G25 of the pre-miR-155 molecule, that contains no secondary structure. When it was hybridized to the array, it bound with equal intensity to all of its complementary oligonucleotides, consistent with the known lack of secondary structure in this short RNA oligomer. Supplementary Figure S2 contains RNA accessible site map for miR-155.

In order to evaluate the effect of RNA concentration upon accessible site determination, the pre-miR-155 array was exposed to various concentrations (1nM to 10 M) of the pre-miR-155 RNA molecule and hybridization was compared. Figure 3 shows the change in SPR signal intensity ( $\Delta\%R$ , the change in light reflected off the array) as a function of RNA concentration. This intensity is directly related to the number of RNA molecules hybridized to the array. Figure 3 shows that the number of RNA molecules hybridized to the array increases greatly for concentrations above 0.1 $\mu$ M (0.2nmols of RNA). Hybridization intensities for RNA concentrations greater than 10 $\mu$ M were not determined, as this amount of RNA is not often available due to cost and/or sample limitations. It is also worth noting that the number of RNA molecules hybridized to the array does not change greatly for concentrations ranging from 1nM to 0.1 $\mu$ M, yet is still significantly higher than the signal intensity of the features that are not

hybridized as well as the background. Unless otherwise indicated, solutions of 1  $\mu$ M (2 nanomoles of RNA) were used for the hybridization experiments presented here.

### Pre-let-7a3 RNA-specific array

The pre-let-7a3 (Table 1) RNA-specific array is a 725-feature tiling array composed of 4mer, 5mer, 6mer, 8mer, and 12mer oligonucleotide features. Figure 1b contains a diagram and reference image of the pre-let-7a3 RNA-specific array before hybridization. Figure 4 shows a difference image obtained after the pre-let-7a3 RNA molecule was hybridized to the array. Hybridization was observed at start position G1 to G3, U24 to G27, and U42 to G46 corresponding to accessible regions of G1 to G8, U24 to U32, and U42 to A50, respectively. When compared to the 6mer features, the 8mer and 12mer features exhibited expanded binding regions with higher signal while the 4mer and 5mer features showed reduced signal and increased specificity. The RNA accessible site maps for 4mer, 5mer, 8mer, and 12mer oligonucleotide probes are shown in Figure S3 in the Supplementary Information. Hybridization of the mature 22mer let-7a miRNA (U4-U25 in pre-let-7a3) showed binding to all of its complements on the array. This again indicates a lack of secondary structure in these short RNA oligomers.<sup>38</sup>

### Pre-let-7c RNA-specific array

The pre-let-7c (Table 1) RNA-specific array is a 502-feature tiling array composed of 6mer, 8mer, and 12mer oligonucleotide features. Figure 1c contains a diagram and reference image of the pre-let-7c RNA-specific array. Figure 5 contains a difference image of the pre-let-7c sequence specific array after hybridization. Hybridization to the 6mer oligonucleotides was observed at start positions C44 to U46 and U47, which correspond to accessible regions of C44 to G51 and U79 to C84. This indicates the presence of accessible sites in the hairpin loop and 3'-end of the stem. However, binding at the 3'-end could also be due to hybridization to the C44-G51 region as they are similar in sequence (7/8 bases). Figure S4 in the Supplementary Information contains accessible site maps obtained from the 8mer and 12mer oligonucleotides.

### Universal RNA array

RNA-specific oligonucleotide arrays must be designed and fabricated for each for specific RNA sequence of interest. It would be useful if a single general-purpose array could be used for any desired RNA of interest. To evaluate this possibility, a universal array composed of all possible 6mer oligonucleotide sequences was fabricated and the hybridization results were compared with those obtained on the RNA-specific array (Figure 4). The universal array is a 4122-feature universal array composed of the 4096 6mer combinations and 26 control features. Figure 6a shows an SPR image of the universal array after hybridization with the pre-let-7a3 RNA molecule. The binding pattern observed on the universal array correlates with that obtained from its RNA-specific array analog.

In addition to the expected hybridization at the 6mer perfect complements on the array, hybridization was also observed at features on the universal array that are mismatched at the 5'-terminal nucleotide. Thus, there are typically four features that bind each 6mer sequence contained within the RNA (the perfectly-matched complements plus three others differing at the 5'-terminal nucleotide). It should be noted that such non-specific hybridization events do not adversely impact the use of universal arrays when generating accessible site maps when the RNA sequence is known, as one can limit the image analysis to only the oligonucleotide complements that are present in the RNA sequence being analyzed. Non-specific hybridization to array features, however, can provide insight into alternative oligonucleotide sequences with varying binding affinities and thus varying physiological effects when utilized in RNAi applications. Figure 6b is a graphical representation of hybridization intensity as a function of the pre-let-7a3 RNA molecule's sequence and Figure 6c the accessible site map. Hybridization



was observed at start positions G1 to G2, U26 to U27, and U42 to A50, which correspond to accessible regions of G1 to G7, U26 to U32, and U42 to A50. The accessible site map obtained on the universal array corresponds well to the accessible site maps generated from the pre-let-7a3 RNA-specific array (Figure 4c). The RNA-specific array contains expanded accessible regions at the 5'-end (G1 to G8, one nucleotide larger) and from U24 to U32 (a three nucleotide increase).

The use of a 6mer universal array is effective in determining the accessible sites of relatively short RNA molecules, as seen above with the pre-let-7a3 (74 nt) molecule. A universal array consisting only of 6mer oligonucleotides would, however, be problematic for determining accessible sites in substantially larger RNA molecules, as the probability of multiple occurrences of the same 6mer sequence increases with RNA length. It would accordingly be necessary to utilize a universal array containing longer oligonucleotides (e.g. all possible 7mers, 8mers, etc) and correspondingly larger numbers of features (16,384 or 65,536, respectively). For example, the probability of an RNA molecule of length  $n$  with equal numbers of A, C, G, and U bases having two identical 6mers is  $(n-5)/4096$ . Thus the probability of any given 6mer being repeated in an RNA molecule composed of 250, 500, and 1000 nucleotides is 6.0%, 12.1% and 24.4%. The probability of finding a repeat in a 1000 nucleotide molecules decreases from 24.4% to 6.1% to 1.5% when the length of the oligonucleotide probes is increased from 6mers to 7mers or 8mers. Thus, a 6mer universal array is only sufficient for RNA molecules under ~100 nucleotides (probability of 2.3%).

The fabrication of universal arrays composed of longer probe lengths is readily accomplished using the *in situ* oligonucleotide array synthesis utilized in this work, although such a study is outside the scope of the present paper.

## Conclusion

A hybridization-based platform for determining RNA accessible sites is presented here. This platform combines *in situ* synthesized arrays fabricated with MAS technology, carbon-on-metal substrates, and surface plasmon resonance imaging detection methods, allowing one to design and fabricate oligonucleotide arrays with a larger number of features on a single substrate and then analyze hybridization to that array in a label-free manner. The accessible sites of three pre-microRNA molecules were determined with RNA-specific arrays. A universal array composed of all possible 6mer oligonucleotides was also designed and fabricated. The accessible sites of one of the pre-microRNA molecules were determined with the universal array and compared to its RNA-specific analog. The agreement in accessible site maps obtained from the RNA-specific and universal 6mer array for the pre-let-7a3 RNA molecule show that universal arrays provide a suitable, general alternative to the RNA-specific arrays for determining RNA accessible sites.

## Supplementary Material

Refer to Web version on PubMed Central for supplementary material.

## Acknowledgments

The authors would like to thank Professor Franco Cerrina (University of Wisconsin Center for Nanotechnology) for his ongoing support and assistance with MAS technology. This work was supported by NIH grants R01HG002298 and R01HG003275. JBM was supported by an NIH NHGRI training grant to the Genomic Sciences Training Program (5T32HG002760). MRL was supported by the University of Wisconsin Industrial and Economic Development Research Program. LMS has a financial interest in GWC Technologies, Inc., which manufactures the SPR imaging instrument employed in this work.

## References

1. Lewis JB, Doty P. *Nature* 1970;225:510–512. [PubMed: 4904262]
2. Uhlenbeck OC, Baller J, Doty P. *Nature* 1970;225:508–510. [PubMed: 5411856]
3. Lima WF, Monia BP, Ecker DJ, Freier SM. *Biochemistry* 1992;31:12055–12061. [PubMed: 1280997]
4. Vickers TA, Wyatt JR, Freier SM. *Nucleic Acids Research* 2000;28:1340–1347. [PubMed: 10684928]
5. Schulman LH, Pelka H. *Biochemistry* 1976;15:5769–5775. [PubMed: 827308]
6. Fire A, Xu S, Montgomery MK, Kostas SA, Driver SE, Mello CC. *Nature* 1998;391:806–811. [PubMed: 9486653]
7. Chendrimada TP, Gregory RI, Kumaraswamy E, Norman J, Cooch N, Nishikura K, Shiekhattar R. *Nature* 2005;436:740–744. [PubMed: 15973356]
8. Wrzesinski J, Legiewicz M, Ciesiolka J. *Nucleic Acids Research* 2000;28:1785–1793. [PubMed: 10734198]
9. Allawi HT, Dong F, Ip HS, Neri BP, Lyamichev VI. *RNA* 2001;7:314–327. [PubMed: 11233988]
10. Zuker M. *Science* 1989;244:48–52. [PubMed: 2468181]
11. Stull RA, Taylor LA, Szoka FC. *Nucleic Acids Research* 1992;20:3501–3508. [PubMed: 1352874]
12. Sczakiel G, Homann M, Rittner K. *Antisense Res. Dev* 1993;3:45–52. [PubMed: 8495105]
13. Mathews DH, Sabina J, Zuker M, Turner DH. *Journal of Molecular Biology* 1999;288:911–940. [PubMed: 10329189]
14. Mathews DH, Disney MD, Childs JL, Schroeder SJ, Zuker M, Turner DH. *Proc. Natl. Acad. Sci. USA* 2004;101:7287–7292. [PubMed: 15123812]
15. Patzel V, Sczakiel G. *Journal of Molecular Biology* 1999;294:1127–1134. [PubMed: 10600371]
16. Walton SP, Stephanopoulos GN, Yarmush ML, Roth CM. *Biotechnol. Bioeng* 1999;65:1–9. [PubMed: 10440665]
17. Mir KU, Southern EM. *Nature Biotechnology* 1999;17:788–792.
18. Duan S, Mathews DH, Turner DH. *Biochemistry* 2006;45:9819–9832. [PubMed: 16893182]
19. Kierzek E, Kierzek R, Turner DH, Catrina IE. *Biochemistry* 2006;45:581–593. [PubMed: 16401087]
20. Luebke KJ, Balog RP, Garner HR. *Nucleic Acids Research* 2003;31:750–758. [PubMed: 12527785]
21. Fodor SP, Read JL, Pirrung MC, Stryer L, Lu AT, Solas D. *Science* 1991;251:767–773. [PubMed: 1990438]
22. Singh-Gasson S, Green RD, Yue Y, Nelson C, Blattner F, Sussman MR, Cerrina F. *Nature Biotechnology* 1999;17:974–978.
23. Lockett MR, Weibel SC, Phillips MF, Shortreed MR, Sun B, Corn RM, Hamers RJ, Cerrina F, Smith LM. *J. Am. Chem. Soc* 2008;130:8611–8613. [PubMed: 18597426]
24. Lockett, MR.; Smith, LM. *Analytical Chemistry*. Vol. 81. ASAP; 2009.
25. Homola J, Yee SS, Gauglitz G. *Sensors and Actuators B – Chemical* 1999;54:3–15.
26. Rothenhausler B, Knoll W. *Nature* 1988;332:615–617.
27. Thiel AJ, Frutos AG, Jordan CE, Corn RM, Smith LM. *Analytical Chemistry* 1997;69:4948–4956.
28. Goodrich TT, Wark AW, Corn RM, Lee HJ. *Methods in Molecular Biology* 2006;328:113–130. [PubMed: 16785644]
29. Mockler TC, Eckler JR. *Genomics* 2005;85:1–15. [PubMed: 15607417]
30. Strother T, Knickerbocker T, Russell JN, Butler JE, Smith LM, Hamers RJ. *Langmuir* 2002;18:968–971.
31. Phillips MF, Lockett MR, Rodesch MJ, Shortreed MR, Cerrina F, Smith LM. *Nucleic Acids Research* 2008;36:e7. [PubMed: 18084027]
32. Guo Z, Guilfoyle RA, Thiel AJ, Wang RF, Smith LM. *Nucleic Acids Research* 1994;22:5456–5465. [PubMed: 7816638]
33. Nelson BP, Grimsrud TE, Liles MR, Goodman RM, Corn RM. *Analytical Chemistry* 2001;73:1–7. [PubMed: 11195491]
34. Zuker M. *Nucleic Acids Research* 2003;31:3406–3415. [PubMed: 12824337]
35. Krol J, Krzyzosiak WJ. *IUBMB Life* 2004;56:95–100. [PubMed: 15085933]

36. Krol J, Krzyzosiak WJ. *Methods in Molecular Biology* 2006;342:19–32. [PubMed: 16957364]
37. Stenberg E, Persson B, Roos H, Urbaniczky C. *Journal of Colloid and Interface Science* 1991;143:513–526.
38. Data not shown

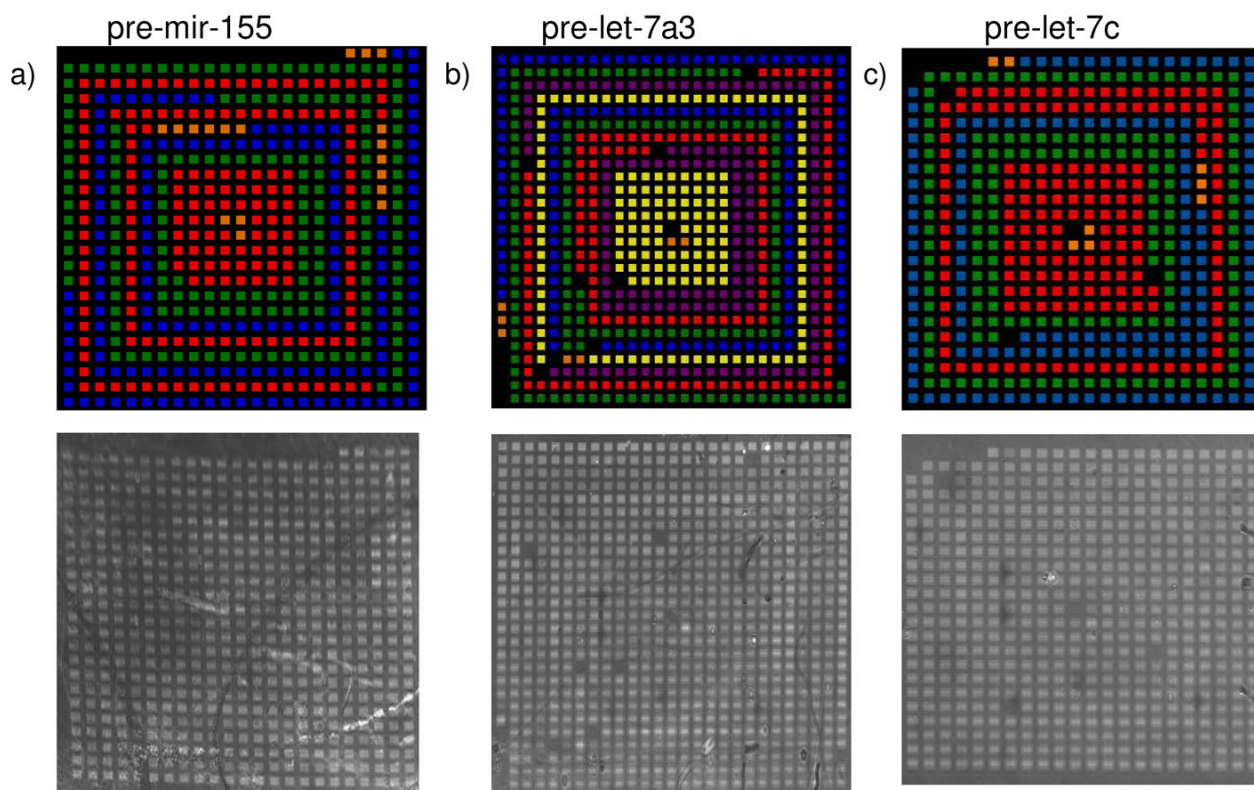


**Figure 1.**

Diagrams (top) and SPR images (bottom) of the three tiling arrays before RNA hybridization. Each array spirals outward from the center base-by-base from 3' to 5'. Black=no DNA, Orange=controls, Yellow=4mers, Purple=5mers, Red=6mers, Green=8mers, and Blue=12mers. a) The pre-miR-155 array has 534 features, b) the pre-let-7a3 array has 725 features, and c) the pre-let-7c array has 502 features. Tables detailing the exact sequences for each feature are provided in Supplementary Tables 1-4.

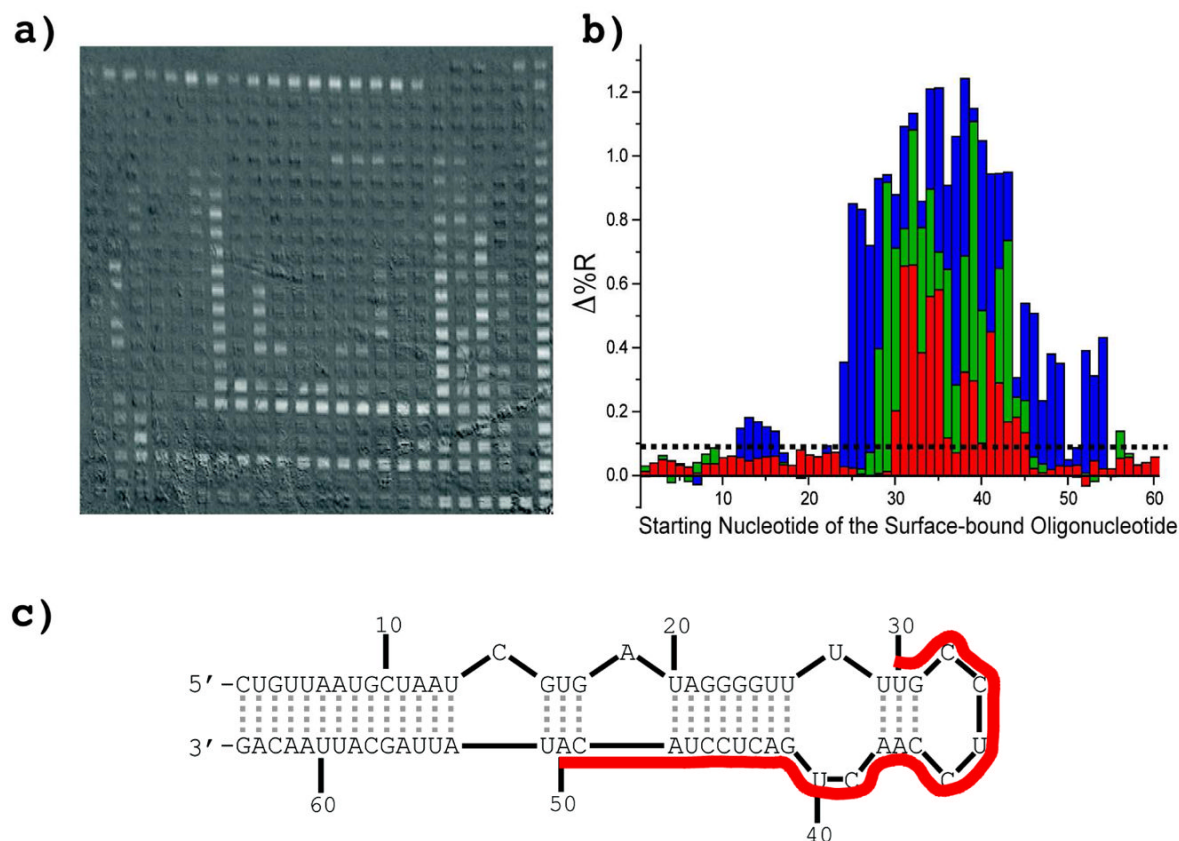


**Figure 2. Pre-miR-155 RNA-Specific Array**

The pre-miR-155 RNA-specific array is a tiling array composed of 6mer, 8mer, and 12mer oligonucleotide features. The array was exposed to a  $1\mu\text{M}$  pre-miR-155 solution and hybridization monitored with SPRi. a) SPRi difference image showing points of hybridization (bright features). b) Histogram of the hybridization data obtained from the difference image. The y-axis corresponds to the average change in % reflectivity ( $\Delta\%R$ ), while the x-axis corresponds to the location of the surface probe along the RNA sequence (Location 1 corresponds to nucleotides 1-6 for 6mers, 1-8 for 8mers, etc.). The red histogram represents the 6mer oligonucleotides, green the 8mers, and blue the 12mers. The dotted horizontal line represents the cutoff line. Features with intensity changes greater than the cutoff line are considered accessible sites. c) The lowest energy structure of pre-miR-155 predicted by Mfold. The 6mer accessible sites determined from the hybridization experiment are indicated by the red line.

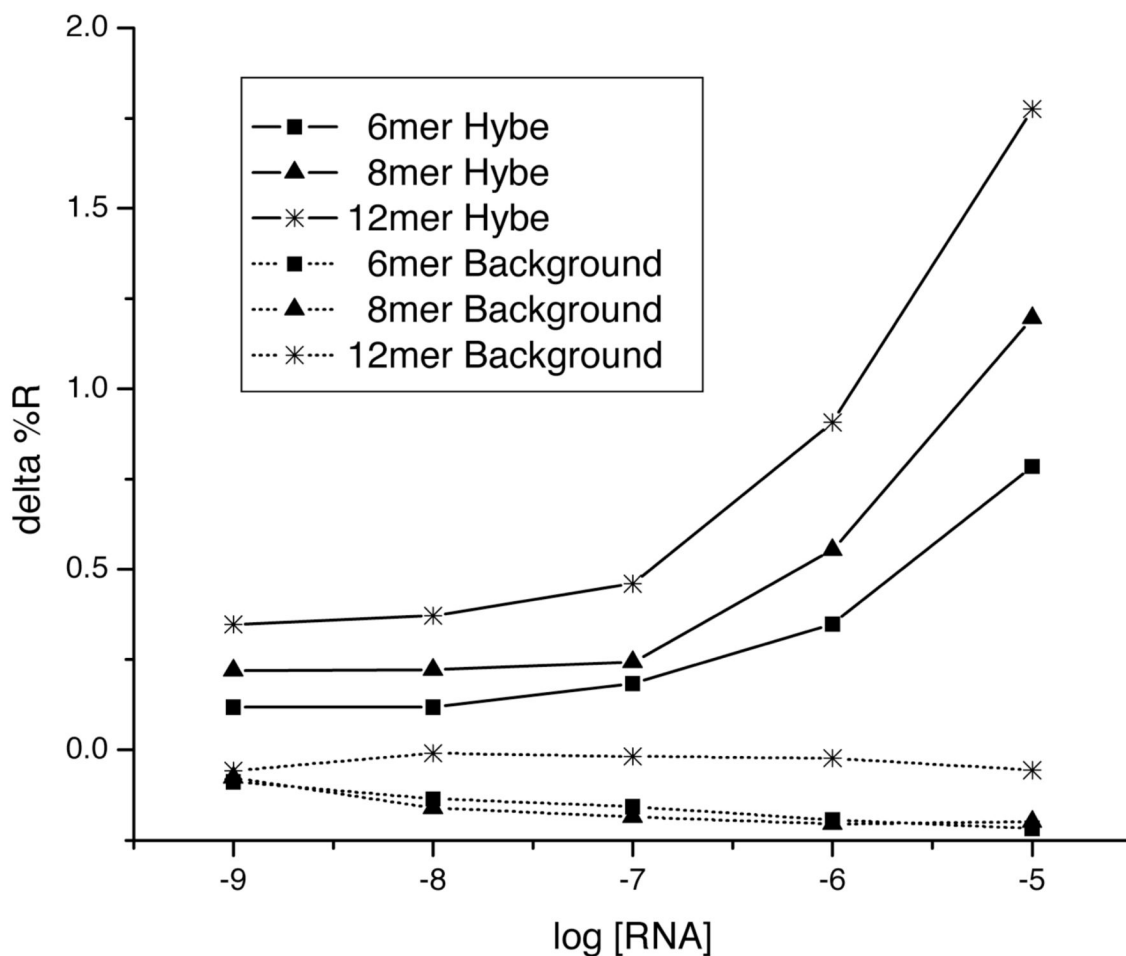


**Figure 3.**

Hybridization of the pre-miR-155 RNA molecule to the pre-miR-155 oligonucleotide array as a function concentration. The three solid lines represent the average of the three probe oligonucleotides with the greatest amount of hybridization (highest  $\Delta\%R$ ) for each probe length. The three dotted lines represent the average of the three probe oligonucleotides with the least amount of hybridization (lowest  $\Delta\%R$ ) for each probe length. Hybridization is observed when as low as 1nM of target is introduced to the array.



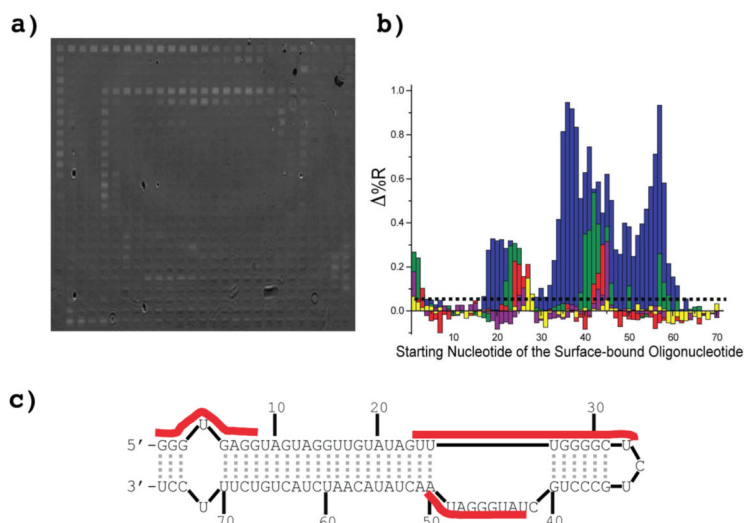


#### Figure 4. Pre-let-7a3 RNA-Specific Array

The pre-let-7a3 RNA-specific array is a tiling array composed of 4mer, 5mer, 6mer, 8mer, and 12mer oligonucleotide features. The array was exposed to a  $1\mu\text{M}$  pre-let-7a3 solution and hybridization monitored with SPRi. a) SPRi difference image showing points of hybridization (bright features). b) Histogram of the hybridization data obtained from the difference image. The y-axis corresponds to the average change in % reflectivity ( $\Delta\%R$ ), while the x-axis corresponds to the location of the surface probe along the RNA sequence (Location 1 corresponds to nucleotides 1-6 for 6mers, 1-8 for 8mers, etc.). The yellow histogram represents the 4mer oligonucleotides, purple the 5mers, red 6mers, green the 8mers, and blue the 12mers. The dotted horizontal line represents the cutoff line. Features with intensity changes greater than the cutoff line are considered accessible sites. c) The lowest energy structure of pre-let-7a3 predicted by Mfold. The 6mer accessible sites determined from the hybridization experiment are indicated by the red line.

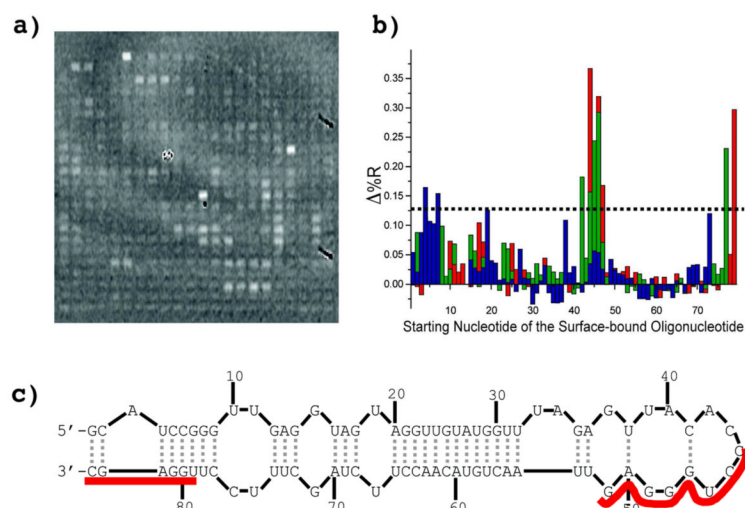


### Figure 5. Pre-let-7c RNA-Specific Array

The pre-let-7c RNA-specific array is a tiling array composed of 6mer, 8mer, and 12mer oligonucleotide features. The array was exposed to a  $1\mu\text{M}$  pre-let-7c solution and hybridization monitored with SPRi. a) SPRi difference image showing points of hybridization (bright features). b) Histogram of the hybridization data obtained from the difference image. The y-axis corresponds to the average change in % reflectivity ( $\Delta\%R$ ), while the x-axis corresponds to the location of the surface probe along the RNA sequence (Location 1 corresponds to nucleotides 1-6 for 6mers, 1-8 for 8mers, etc.). The red histogram represents the 6mer oligonucleotides, green the 8mers, and blue the 12mers. The dotted horizontal line represents the cutoff line. Features with intensity changes greater than the cutoff line are considered accessible sites. c) The lowest energy structure of pre-let-7c predicted by Mfold. The 6mer accessible sites determined from the hybridization experiment are indicated by the red line.

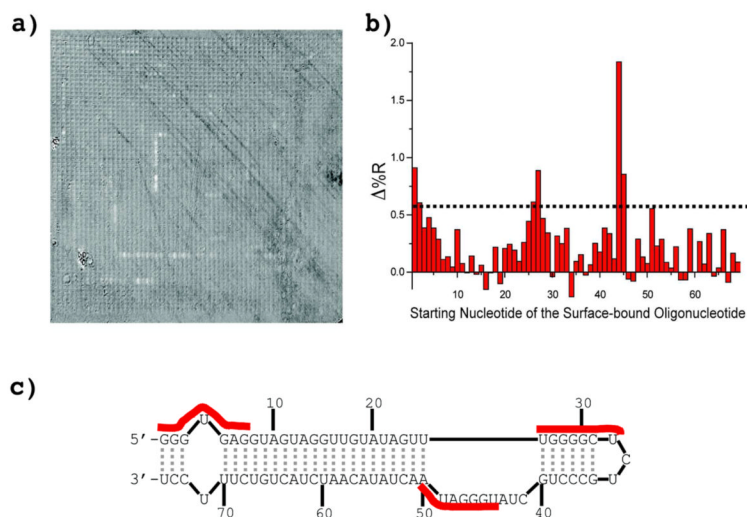


**Figure 6. Universal Array**

A universal array consisting of all possible 6mer combinations was exposed to a  $1\mu\text{M}$  pre-let-7a3 solution and hybridization to the array monitored with SPRi. a) SPRi difference image showing points of hybridization. b) Histogram of the hybridization data obtained from the difference image. The y-axis corresponds to the average change in % reflectivity ( $\Delta\%R$ ), while the x-axis corresponds to the location of the surface probe along the RNA sequence (Location 1 corresponds to nucleotides 1-6). The dotted horizontal line represents the cutoff line. Features with intensity changes greater than the cutoff line are considered accessible sites. c) The lowest-energy structure of pre-let-7a3 predicted by Mfold. The 6mer accessible sites determined from the hybridization experiment are indicated by the red line.

**Table 1****DNA and RNA sequences**

The first five sequences shown correspond to the 5 RNA targets investigated in this work. The next five sequences correspond to the DNA oligonucleotides employed. The Controls are all probes attached to the surface (indicated by --|). Complement 1 and 2 are perfect complements to Control 1 and 2, respectively, excluding the 10 dT spacer sequence.

Name	Sequence (5' -> 3')
pre-miR-155	CUGUUAAGCUAAUCGUGAUAGGGGUUUUUGCCUCCAACUGACUCCUACAUAUUAGCAUUAACAG
pre-let-7a3	GGGUGAGGUAGUAGGUUGUAUAGUUUGGGGCUCUGCCUGCUAUGGGGAUAACUAUACAAUCUACUGUCUUUCCU
pre-let-7c	GCAUCCGGGUUGAGGUAGUAGGUUGUAUGGUUUAGAGUUAACACCCUGGGAGUUAACUGUACAACCUUCUAGCUUCCUUGGAGC
miR-155	CUCCUACAUAUUAGCAUUAACA
let-7a	UGAGGUAGUAGGUUGUAUAGUU
Control 1	ACTCTTGCAGGTCATCGGTTTTTTTTTT--
Control 2	TCACTGTTGCAAAGTTATTGTTTTTTTTTT--
Control 3	Cy3-TTTTTTTTTT--
Complement 1	ACCGATGACCTGCAAGAGT
Complement 2	CAATAACTTTGCAACAGTGC